Monte-Carlo Simulations of BOLD Background Gradient Contributions in Diffusion-Weighted fMRI— Comparison of Spin Echo and Twice-Refocused Echo Sequences

A. Pampel[1], T. H. Jochimsen, [1], and H. E. Moeller, [1]

[1]Nuclear Magnetic Resonance Unit, Max Planck Institute for Human Cognitive and Brain Sciences, Leipzig, Germany

Introduction. Because of its proposed potential to better localize neuronal activity and to observe activation through a mechanism different from the BOLD effect, diffusion-weighted fMRI (DFMRI) has drawn much attention [1-5]. Data from studies using lower *b*-values indicate an increase of the apparent water diffusion coefficient (ADC) during functional activation, which is thought to be caused predominantly by increased blood flow and/or relative volume of intravascular spins with relatively high ADC. Strong diffusion weighting (high *b*-value) primarily detects signals of extravascular origin. In this regime, a minute decrease of the ADC accomplished by a different temporal characteristic compared to the BOLD response was observed. The transient increase of the diffusion-weighted signal, whereby the percent signal change ($\Delta S/S_0$) rose with increasing *b*-value, was attributed to intracellular processes preceding the hemodynamic response [1,2].
Presently, there is still debate about the size of the effect, its observability and its true origin [3-5]. One issue that needs to be discussed due to its impact on any observation of ADC changes is the interaction ('cross-terms') of the diffusion-weighting (DW) gradients and susceptibility-induced background gradient fields around vessels [4]. Dedicated sequences exist that permit suppression of cross-terms by optimized schemes of sign-alternating DW gradients [6]. However, effective cross-term compensation is prevented if the background gradient contributions are non-linear and/or varying during the time course of the sequence. In case of rapidly varying background gradients 'visited' by the molecules, the spin phases accumulated under the influences of DW and background gradients are independent of each other. As a result, background gradients act as a mechanism that accelerates overall signal attenuation. In case of an intermediate motional regime a general predication cannot be made easily. However, it seems reasonable to assume that interactions between background gradients and DW gradients cannot be suppressed completely. As a consequence, it is necessary to survey the signal formation under the real conditions of the experiment [7]. Here, we investigate by Monte-Carlo (MC) simulations, to what extent couplings between background gradients of vascular origin and DW gradients could influences the extravascular DFMRI signal changes observed by the popular Twice Refocused Echo Sequence (TRE) [8].

Theory and Methods. The parameters of the TRE sequence were adapted to null cross-terms between DW and (linear) background gradients. MC simulations that integrate the Bloch equations numerically for a large number of random walks were performed to calculate the signal of molecules diffusing in a vascular network. We used a well-established vascular model that describes the brain vasculature as an arrangement of randomly oriented, infinitely long cylinders of variable size [9, 10]. The shift of frequency around a vessel is $\Delta\omega = -0.5\ \gamma\Delta\chi B_0\rho^2 r^{-2}\cos 2\varphi \sin^2\theta$ (cylinder radius ρ, distance from the center of the cylinder r, susceptibility difference $\Delta\chi$, magnetogyric ratio γ, magnetic field B_0). It is assumed that blood has an equivalent susceptibility given by $\Delta\chi = HCT(1-Y)\chi_{dHb}$ (*HCT* hematocrit, *Y* fractional oxygenation, χ_{dHb}=2.26 ppm susceptibility of deoxyhemoglobin). Simulations were carried out using blood/tissue susceptibility difference ($\Delta\chi$), corresponding to the typical values used to compute BOLD susceptibility changes: resting state: *Y*=0.6, $\Delta\chi$=0.36 ppm; activated state: *Y*=0.8, $\Delta\chi$=0.18 ppm [11]. As an intermediate value, cerebral blood volume fractions (CBV) of 2% were considered in the simulation. It is sufficient to perform the simulation in two dimensions, namely in those which span the plane perpendicular to the cylinder axis. To simplify simulations, a periodic pattern was assumed with the cylinder placed in the center of each quadratic cell of the pattern. For each radius, 10^9 vessel orientations (θ) were randomly chosen from the interval 0 to $\pi/2$, and a random walk was computed. The starting position was chosen randomly with a uniform distribution throughout the cell. The displacement at each step for the random walk was generated by a Gaussian distribution with zero mean and variance $2D\delta t$ in each (cartesian) dimension. A diffusion coefficient of D=7.6·10^{-4} mm^2/s was assumed to match that of gray matter. To simplify the simulation algorithm, vessel walls were considered to be fully permeable. Because intravascular signal is neglected in this study, the signal of a particle was discarded when inside the vessel. At each step of duration δt=0.25 ms, the local Larmor frequency at 3 T plus the local field caused by the DW gradients was used to calculate the phase shift. The gradient strengths were adapted for diffusion weighting using *b*=0, 600, 1200, 1800, and 2400 s/mm^2, respectively. *TE* was 100 ms in all simulations. Simulations were performed at vessel radii varying from 2-100µm, respectively. The signal was created summing up the calculation for the respective radii after weighting using a distribution described in [9]. For comparison, simulations of the Stejskal-Tanner spin-echo experiment (SE) were performed using equivalent conditions.

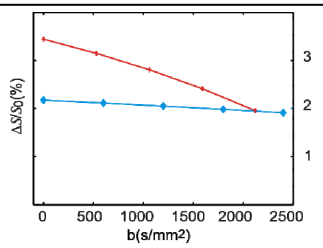

Fig. 1. ($\Delta S/S_0$) in dependence on *b*-value; TRE (blue), SE (red).

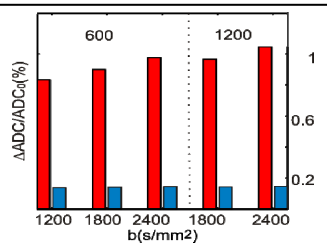

Fig. 2. ($\Delta ADC/ADC_0$) in dependence on *b*-value. TRE (blue), SE (red), obtained with b_1=600 or 1200 s/mm^2.

Results and Discussion. Simulated ($\Delta S/S_0$) obtained during stimulation (i.e. change of *Y*) is presented in Fig. 1. The TRE sequence shows a rather weak decrease with increasing *b*-value, i.e. it can almost completely suppress the cross-term distribution. The SE sequence shows a decrease of ($\Delta S/S_0$) in dependence of *b*, which can be attributed to cross-terms. As expected from the longer refocusing periods compared to TRE, ($\Delta S/S_0$) is larger at smaller *b*. In Fig. 2, the relative changes of ADC as calculated form the data are shown. The ADC was calculated by ADC = $[b_1\text{-}b_2]^{-1}\cdot\ln[S(b_2)/S(b_1)]$ and setting b_1=600,1200 s/mm^2. Again, almost no dependence on *b* is observed for the TRE sequence, whereby a slight increase of $\Delta ADC/ADC_0$ is observed for the SE sequence. Here we have neglected the influence of intravascular signal contributions which is justified accounting for the b-values (>600 s/mm^2) used.

Conclusions. The simulations demonstrate that the TRE sequence, if adapted to suppress cross-terms to linear background gradients, sufficiently suppresses interactions of the DW gradients and susceptibility induced (background) gradients of vessels under similar conditions used in former studies [2,3]. As expected, such interactions are readily seen in data derived with the SE sequence. If TRE is used with parameters that violate the condition for cross-term suppression, the size of the impact of the cross-term has to be simulated again, but this size will be in the range between those observed with SE and TRE. It was found, that modifications of physiological parameter used for the simulation (CBV, $\Delta\chi$, weighting function) do not change the general conclusion, but moderately modify the absolute values shown in Figs. 1-2. Cross-terms between DW and background gradients are not causing an ADC decrease during neuronal stimulation, independent of the type of sequence used. Nevertheless, the quantities found for $\Delta ADC/ADC_0(b)$ have to be taken into account when interpreting data of DFMRI experiments.

References: [1] Darquie et al., PNAS 98(16):9391 (2001); [2] LeBihan et al, PNAS 103:8263 (2006); [3] Miller et al., PNAS 104(52):20967 (2007); [4] Yacoub et al., MRM 26:889 (2008); [5] Goerke et al., JMRI 25:947 (2007); [6] Zheng et al., Concepts in NMR, 30A(5):261 (2007); [7] Kärger et al., Adv. Magn. Reson. 12:1 (1988); [8] Reese et al., MRM 49:177 (2003); [9] Jochimsen et al., NeuroImage 40:228 (2008); [10] Fisel et al., MRM 17:336 (1991); [11] Marques and Bowtell, NMR in Biomed. 21(6):553 (2007).